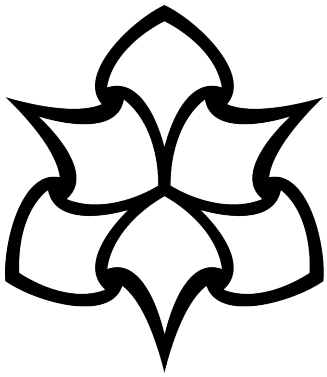

Biophysical Chemistry 297 (2023) 107010

Contents lists available at ScienceDirect

Biophysical Chemistry

journal homepage: www.elsevier.com/locate/biophyschem

pH-equilibration of human hair: Kinetics and pH-dependence of the partition ratios for H^+ – and OH^- -ions based on a Freundlich isotherm

Franz J. Wortmann [a,c,*], Katie Hardie [a,1], Natalja Schellenberg (nee Focht)[a,b,2], Celina Jones [a], Gabriele Wortmann [a,c], Erik Schulze zur Wiesche [b,3]

[a] Department of Materials, School of Natural Sciences, The University of Manchester, UK
[b] Henkel AG & Co. KGaA, Hamburg, DE.
[c] F & GW – Consultants, Aachen, DE

ARTICLE INFO

Keywords:
Human hair
pH-equilibration
Kinetics
Ion partition ratios
Freundlich isotherm

ABSTRACT

Hair is an insoluble, fibrous, α-keratinous, protein composite material, providing outer coverage, e.g., for mammals. In the context of a wider study on the effects of pH on human hair properties, we investigated the time-dependence of pH-equilibration study across the acid and the basic pH-range, using appropriate pure solutions of hydrochloric acid and sodium hydroxide. The results show that pH-equilibration follows essentially equal 1st-order kinetics across the pH-range. The characteristic process time does not change significantly and is in the range of 2.5–5 h. The analysis enables to determine the equilibrium uptakes of H^+- and OH^- -ions. These follow the expected U-shaped path across the pH-range. For both acidic and alkaline conditions, data are well described by two very similar sorption isotherms of the Freundlich-type. In consequence, partition ratios for both ions are highest near neutrality (pH 7: >6000) and drop off strongly towards low and high pHs (<50). Hair is thus a very strong 'sink' for H^+ and OH^-. This observation fundamentally challenges traditional views of limited ion uptake, namely, in the mid-pH-range due to hindered diffusion. It also does not support considerations on special roles of certain pHs, specific groups of amino acids, or morphological components. Our analysis thus suggests that established views of the interaction of hair and pH need to be reconsidered, The Freundlich isotherm approach appears to provide a versatile tool to refine our understanding of the interactions of hair and possibly other keratinous materials (horn, nail, feathers) with acids and bases.

1. Introduction

Human hair is a complex biological composite material. It is part of a larger group of keratins, which form the outer covering of higher vertebrates (hair, horn, nail, hoof, feather). As such they have a wide range of principal functions ([1], [2]). The main components of the hair structure are an outer protective layer (cuticle, ≈ 10% of fibre material) and a fibre core (cortex, ≈ 90%). The cortex is essentially a fibre/matrix composite, comprising partly α-helical intermediate filaments (IF) embedded in amorphous IF-associated material ([3]; [1]; [4];). All of these components contain a wide variety of proteins with individual amino acid sequences to enable specific secondary, tertiary and quaternary structures [5,2,6]. The amino acids may be grouped according to the nature of their side-groups as being acidic, basic or neutral [6]. There are approximately equal amounts of negatively and positively charged amino-acids, providing electric neutrality [4,7,8].

With the high amounts of acidic and basic side-groups in the proteins of hair, the pH of the liquid environment, when treating human hair in a cosmetic context, has a profound impact on the physical and chemical properties of the fibres as well as on the outcome of the specific treatment [4]. This includes effects from interactions with a wide variety of electrolytes, charged polymers etc., which are applied in cosmetic processes and products ([9]; [10,11]; [12]; [13,14]).

The basis of the effects of acidic or basic pH on the hair proteins in an aqueous environment may be seen as physi-sorption of the ions according to the following two, basic schemes [15,16]:

* Corresponding author at: Department of Materials, School of Natural Sciences, The University of Manchester, M13 9PL, UK.
E-mail address: franz.wortmann@manchester.ac.uk (F.J. Wortmann).
[1] Current address: MAIC Europe Ltd., Manchester, UK.
[2] Current address: Haupt Pharma Muenster GmbH, Muenster, DE.
[3] Current address: Dr. Kurt Wolff GmbH & Co KG, Bielefeld, DE.

https://doi.org/10.1016/j.bpc.2023.107010
Received 29 January 2023; Received in revised form 18 March 2023; Accepted 23 March 2023
Available online 25 March 2023

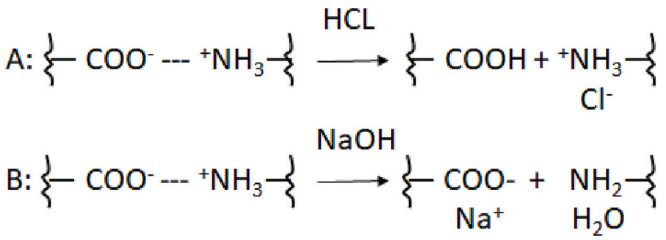

Fig. 1. A: Breaking of the 'salt links'(—) between an anionic and a cationic side- or end- group with a strong acid (HCl). B: As (A) but for a strong base (NaOH) (adapted from [15]).

The left-hand sides of Eqs. 1A and 1B in Fig. 1 describe the so-called 'salt-link' [17]. It is also referred to as 'Coulombic'- [3,18] or simply as 'ionic' -interaction'. This type of interaction plays an important role for the stability and properties of the structures of hair on all levels [3]. The ionic interactions are broken by acid or base (right side of Eqs. 1A and 1B in Fig. 1).

The rate constants for the reactions in Fig. 1 as well as the extent of each at a given pH will depend on a variety of factors. The most important of these are expected to be the specific pK_As of the side groups of the amino acids with a further, comparatively small contribution from the protein end groups [15,19]. In view of Eqs. 1A and 1B (see Fig. 1), we consider the processes for H^+ and OH^- -uptake, primarily, as physisorption, driven by ionic interactions.

Over a rather wide range of pH on both sides of neutrality (approx. > ≈ pH 4 – <≈ pH 10) fibres take up little H_3O^+ –, or more simply H^+ –, as well as OH^- -ions [15,4]. This range was originally referred to as 'isoelectric or neutral range' [15,4]. This special behaviour [4] is generally associated with hindered diffusion for the ions in that range, which is overcome, namely, on the acid side around the isolectric point (pH 2.5–4.5; [20]; [21]; [22]).

The traditional and simple way to study the interaction of keratin fibres, such as wool and hair, is to immerse the sample in an aqueous solution of known pH and then to determine the pH after equilibration. [17]. With a specific emphasis on wool textile processing, these studies were, e.g., done for a variety of strong acids [23] and under the influence of salts [24] and at different temperatures [25]. An intensive discussion was held in the 1940 – 60s on theories to, namely, explain and model the effects seen in a wide variety of experiments [15,7], as more recently reviewed by Lewis and Rippon [26].

Studies on hair followed much later and remain comparatively scarce. These were usually done using automatic titration technology to follow changes of H^+- and OH^-- ion concentrations at constant pH [27,28].

In the context of a wider investigation on the effects of pH on hair [29,30], we found that there was little quantitative data on the time-dependence of pH-equilibration. We aimed at a suitable experimental process to obtain hair samples with well-defined uptakes of H^+- as well as OH^- -ion samples, as basis to study pH-related changes of hair.

For our studies, we furthermore required an analytical model for the relationship between pH of the immersion solution and H^+ or OH^--uptake of hair.

In view of the experimental simplicity [17,31], we opted for the pH-equilibration method ([32]; [30]). When immersing a hair tress into an aqueous solution of defined pH, pH-changes could be easily monitored either continuously or discontinuously at appropriate points in time.

The data by Hardie [30] were the basis to model the time-dependence of pH-equilibration. These were supplemented by experimental data for equilibration pH after 24 h [29]. These turned out to effectively reflect equilibrium conditions, determining the final uptake of hydrogen as well as hydroxyl -ions into hair for a given aqueous pH. This enabled to determine the pH-dependent partition for H^+ and OH^- between the solid (hair) and the liquid (aqueous phase), leading to a plausible alternative to the traditional analytical models for the sorption of the ions [15,26,7].

2. Materials, methods and basic results

2.1. Hair material

All experiments [29,30] were conducted on commercial, medium brown, untreated, Caucasian hair (Kerling International, Backnang, Germany). The material was used in the form of 20 cm long tresses. 1 g (± 0.002 g) of tress material was taken from a larger bulk and tied in the middle with a polyester thread. The material was standardised by immersion into 1 L of de-ionised water (pH 6.3) for 24 h under constant shaking (30 rpm). Subsequently, the tress was left to air-dry under ambient conditions (approx. 22 °C, 50% relative humidity). The results of the subsequent pH-equilibration experiments were not adjusted for changes of tress weight due to water up-take. Under ambient room conditions, hair is expected to contain about 10–12% water (regain). Upon immersion in water, uptake is expected to rise to about 25% [4,33]. Using ambient conditions as reference for the state of hair is common practice in hair cosmetic research to aid experimental simplicity and consistency.

2.2. pH-equilibration

A hair tress, after the standardisation treatment, was placed into a beaker containing HCl- or NaOH –solution of adjusted pH ([30,32]). Nitrogen was used to provide and maintain an inert atmosphere above the solution. Samples were maintained at 25 °C and under constant mild shaking (30 rpm). The mechanical movement of the tress in the solution ensured material immersion and wetting during the experiment. The pH of the solution was monitored over a period of 24 h. Data were retrieved intermittently and at times being approximately equidistant on a log-time scale. Experiments were conducted at a high liquor ratio (HLR) (1 g hair/1 L) for the pH-range around neutrality (approx. pH 4–7 and pH 7–8), that is at low H^+- and OH^- -concentrations. To ensure that at lower and higher pHs and thus higher ion concentrations changes of pH could be determined, a low liquor ratio (LLR) was used (1 g hair/100 mL). Both liquor ratios were used for pH 4 and pH 8. Experiments were conducted at least in duplicates. In prior experiments [29] initial and final pH (after 24 h) of a solution were determined for LLR-condition at room temperature (24 ± 3 °C) and for pH 1.6 – pH 12. Tests were in conducted in duplicates, under inert atmosphere and with mild stirring.

We do not expect relevant acid hydrolysis of hair proteins for the chosen conditions [5,7]. However, the situation will be somewhat different for alkaline conditions, namely, above ≈pH 10 [34,15,7]. We discuss this matter below in qualitative terms but have not taken it into quantitative considerations [25] at this stage of our investigation.

2.3. Basic equilibration curves

Figs. 2 and 3 shows typical pH(log t) –data for HLR- and LLR-experiments in the experimental range. For both pH-ranges, the data show an overall sigmoid course. Through H^+- and OH^- -ion absorption by hair, pH rises for acidic (see Fig. 2) and falls for alkaline conditions (see Fig. 3), respectively. The lines through the data points are fits according to Eq. (1), as introduced below.

Between approximately pH 4 and pH 9, HLR-conditions are suitable to obtain data that follow with log-time sigmoid curves from a lower to a higher pH, describing the time-dependent absorption of the ions by the hair from its aqueous environment. Outside this range, pH-change needs to be enhanced by switching to LLR-conditions.

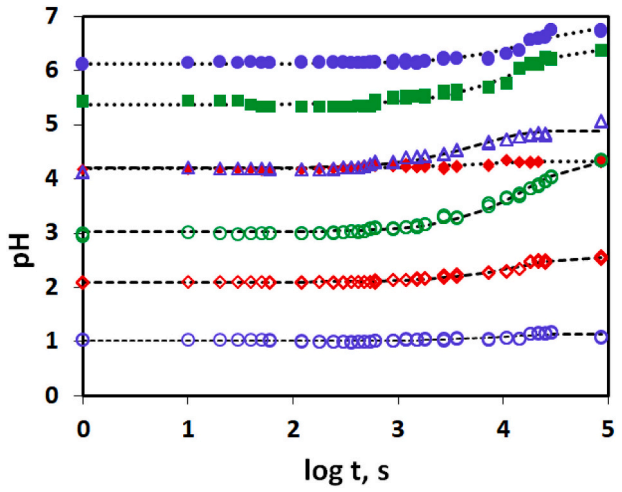

Fig. 2. *pH* vs *log t* for the experimental acidic pH-range. HLR: solid symbols; LLR: outlined symbols. The lines through the HLR (…) and LLR (- - -) -data are fitted on the basis of Eq. (1), using the parameter values underlying Figs. 4 and 7.

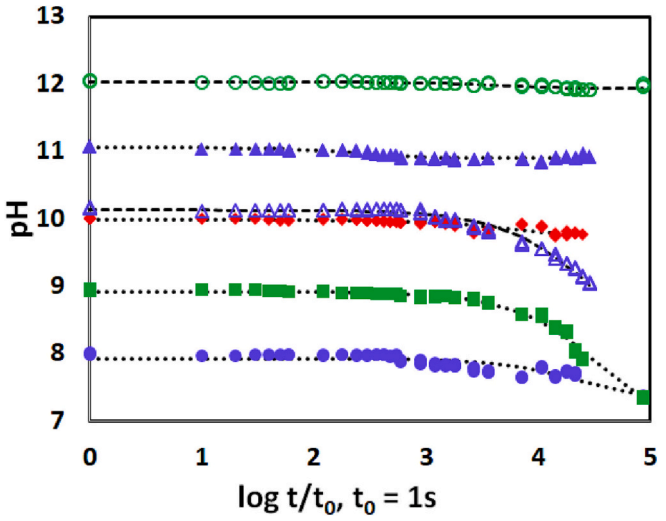

Fig. 3. *pH* vs *log t* for the experimental alkaline pH-range. HLR: solid symbols; LLR: outlined symbols. The lines through the HLR (…) and LLR (- - -) data are fitted on the basis of Eq. (1), using the parameter values underlying Figs. 4 and 8.

2.4. Principles of pH-curve analysis

Upon immersion and depending on the pH of the surrounding solution, the hair tress will start to absorb either H^+ (or rather H_3O^+) or OH^- -ions, together with the respective counter ions. The extent of the absorption process will primarily depend on the pH of the solution. However, temperature [25] and additional electrolyte also play an important role [31].

pH-equilibration may be viewed as a kinetic relaxation experiment [35]. From the shapes of the pH(log t) curves in Figs. 2 and 3, we consider it as a reasonable starting point [36] to assume that the data may be described as a simple exponential, 1st order type kinetic process [37].

As shown in Fig. 2, there is a sigmoid up-turn of the curves for acid conditions from a start pH (pH_0) towards an equilibrium pH (pH_∞). This behaviour is mirrored for alkaline conditions, where curves start at pH_0 and decrease towards pH_∞. This leads us to propose the following 1st-order type equation for the description of the data in Figs. 2 and 3, which leads to appropriately sigmoid curve fits on the log-time scale:

$$pH(t) = pH_\infty + (pH_0 - pH_\infty)\ exp\ (-t/\tau) \quad (1)$$

where τ is the characteristic equilibration time.

All data sets were fitted with Eq. (1), using the Solver-function in Excel (Microsoft, 2016) by minimising the total sum of Squared Errors (SS). The analysis showed that the coefficient of determination, giving the fraction of *SS* explained by the fit, is for most curves above $R^2 \geq 0.8$. However, namely near the limits of the experimental range, as defined either by quite high (≥ 10), low (≤4) pH or close to neutrality, the goodness of the fits decreases, reaching for one data set only $R^2 = 0.07$ (pH 7.5). From correlation analysis [38], we estimated that curve fits for data set of $N > 65$ would be significant on the 95%-level for about $R^2 \approx > 0.1$. This approach was confirmed by fitting specific curves using the Non-linear Estimation tool of Statistica (V13, Tibco Software, 2018) to check whether all parameters were statistically significant on 95%-level beyond $R^2 > 0.1$. According, only the one data set needed to be removed from the data pool.

We are well aware that Eq. (1), despite its success to model the experimental data, represent an essentially empirical approach to describe the pH-equilibration of hair. However, more complex considerations of this matter [16,37] are outside the scope of the current investigation.

3. Results

Fig. 4 summarizes the results for the characteristic equilibration time, which in view of the structure of Eq. (1) is given as log (τ) for HLR- and LLR -conditions.

Table 1 gives the arithmetic means for *log* τ, the related standard deviations as a measure of precision and the 95%-confidence ($q_{95\%}$) range for the 95%-confidence limits for the characteristic equilibration time on the linear time scale.

Analysis of variance shows that, the means are significantly different on the 95%-level ($p = 0.005$). HLR and LLR data are similarly well normally distributed, as seen in normal probability plots. However, means are less than one standard deviation apart with the 95%-ranges overlapping. The overall mean yields on the 95%-level a characteristic relaxation time between $9.4*10^3$ s and $18.6*10^3$ s across the pH-range, which gives an overall range of 2.6–5.2 h. In view of the scatter of the results for log τ (see Fig. 4), we did not consider further analyses, such as linear regression. Based on the overall mean for *log* τ, 50% of the pH-change will have been completed after $t_{50\%} = 8.7\ *10^3$ s (≈ 2.4 h).

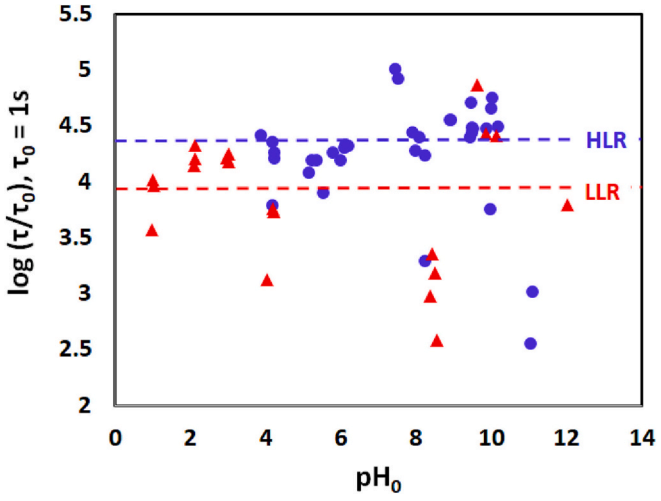

Fig. 4. Characteristic equilibration times, as *log* τ, for HLR (● 1 L)- and LLR (▲0.1 L)- conditions versus initial *pH* (pH_0). The broken lines give the arithmetic means across the pH-range for both conditions. For details see Table 1.

Table 1
Arithmetic means for the characteristic equilibration times, as *log τ*, for HLR (1 L)- and LLR (0.1 L)- conditions. *StdDev* = standard deviation. *N* = number of data points. $q_{95\%}$ = 95%-confidence interval. $Min_{95\%}$ and $Max_{95\%}$ = lower and upper limits of the 95%-interval, respectively, for the linear time scale.

	log τ, s (Mean)	StdDev (N)	$q_{95\%}$	τ, 10^3 s $Min_{95\%}$	τ, 10^3 s $Max_{95\%}$
HLR	4.3	0.47 (34)	0.16	12.9	27.4
LLR	3.9	0.57 (20)	0.27	7.2	13.4
Overall	4.1	0.54 (54)	0.15	9.4	18.6

After about 16 h the process will have progressed to 99% conversion, being essentially complete after 24 h.

As reason for this difference between the liquor ratios, we hypothesise that the mild shaking conditions may not have been quite sufficient to ensure complete homogeneity of the solution throughout the experiment, namely, at the fibre surface.

Fig. 5 summarizes the overall changes of pH ($\Delta pH = pH_0 - pH_\infty$) versus initial pH ($pH_0$) for all experimental HLR- and LLR- curves, as estimated on the basis of Eq. (1). In the context of a separate investigation Focht [29], as outlined above, determined pH-changes for LLR-conditions after 24 h of equilibration. Since after this time pH_∞ -conditions are essentially reached, these data are incorporated into the LLR-data set in Fig. 5. The lines through the HLR (···) - and LLR (––) - data sets in Fig. 5 for both acidic and basic conditions are determined on the basis of the straight-line fits in Figs. 7 and 8, for which the parameter values are given in Table 2.

4. Discussion

4.1. pH-curves

Figs. 2 and 3 summarise the sigmoid pH-equilibration curves for HLR- as well as LLR – conditions and across the experimental pH-range. As the curves through the data document, Eq. (1) is in all cases well suited to fit the time-dependence of the pH-equilibrations. As we expected, there is an increase of pH in the acid and a corresponding decrease in the alkaline region.

4.2. pH-equilibration time

We observe that the time parameter τ (as *log* τ), which characterises the pH-equilibration process (see Eq. (1)), is essentially constant at between approximately 3–5 h across the experimental range (see Fig. 4 and Table 1). Qualitatively, this invariance corresponds to that of the relative velocity constant for H^+- and OH^- -uptake, as determined by Bhat et al. [27] on the basis of short-time ($\leq$ 20 min) titration curves. However, quantitatively there is a large difference between the time scales for equilibration. This is achieved after $\approx$ 16 h for the pH-change (see above) while it is estimated to take only $\approx$ 30 min to 1 h for H^+ as well as OH^- -uptake [27,15,3,7]. This apparent difference is attributed to the fact that ΔpH is a logarithmic measure compared to the corresponding linearly scaled ΔH^+ and ΔOH^- -changes. We thus expect changes of H^+ and OH^- to follow different [37] and much faster kinetics, in line with experimental observations [27,15]. The correspondence between the kinetics of pH-change and ion – uptake merits, in our view, further investigations.

4.3. Equilibrium uptake of H^+- and OH^-- ions by hair

From the results shown in Fig. 5 we calculated the concentrations of H^+- and OH^- -ions [μM/mL] in the various solutions at equilibrium. This yields by comparison with the initial concentrations, as given by pH_0, the uptake of the ions into the hair [μM/g]. The 'diluted solution' -approach appears justified for the experimental range of pH 1-pH 12, since the activity coefficients for H^+ (or rather H_3O^+) and OH^- are both >0.9 [39]. On this basis, the results corresponding to the data points in Fig. 5 are summarized and plotted against equilibrium pH (pH_∞) in Fig. 6. Equilibrium pH was chosen for the x-axis so that literature data could be readily included.

To put our results into perspective, we supplemented them in Fig. 6 with data for wool and hair from three literature sources for roughly comparable experimental conditions [27,40,25]. The data in Fig. 6 are fitted by curves through both the HLR and LLR-data. The curves and their respective 95%-confidence limits are calculated on the basis of the regression lines shown in Figs. 7 and 8, and their parameter values (see Table 2). Fig. 6 shows that the data from different sources overall integrate well with our observations, namely, for acidic conditions.

Overall, the data follow the expected U-shaped curve with strong upward turns starting around pH < ≈4 in the acid and at pH > ≈10 in the alkaline region, respectively. If OH^- -uptake data would be plotted

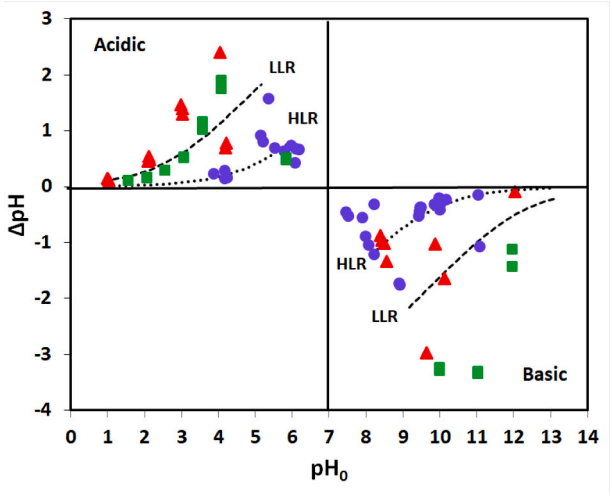

Fig. 5. ΔpH-values are plotted versus pH_0, as obtained by fitting Eq. (1) to the experimental data [30] for HLR (● 1 L)- and LLR (▲ 0.1 L)- conditions. Data are supplemented by those from 24 h LLR pH-equilibration experiments (■ 0.1 L; [29]). For details on the fits through the HLR (···) - and LLR (––) - data sets for both acidic and basic conditions see text. Levels for zero pH-change as well as for neutrality (pH 7) are marked by solid lines.

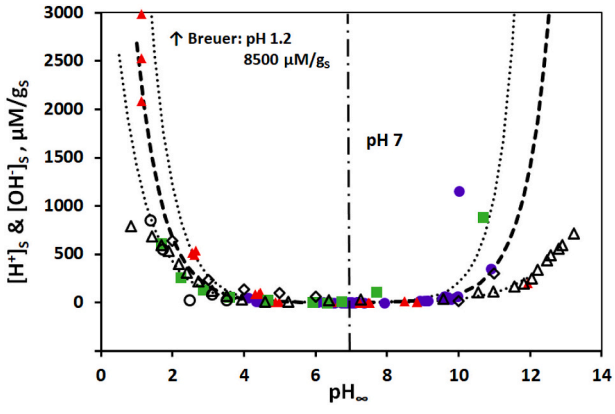

Fig. 6. Data for H_S^+ - and OH_S^- uptake into hair (solid) versus equilibrium pH (pH_∞) for both liquor ratios [30] HLR (●), LLR (▲), Focht [29] LLR (■). Unit [μM/g_s] = μMole per g of solid hair. The line through the data (– – -) is fitted for HLR- and LLR- conditions based on Eqs. (3) and (5). 95%-confidence limits for the fit in the acid and basic region are given (····). The solid horizontal line marks the y = 0 level. The Figure is supplemented by literature data (**Δ**: [25]; **O**: [40]; ◊: [27]). Literature data are not part of the data fit. Neutrality pH (pH 7) is marked.

on a reverse scale, they would show together with the H^+-data the tilted sigmoid form of the titration curve for wool and hair with acids and bases [27,15,41,4,17].

While our data follow a common trend in the acid range, they show considerable scatter in the alkaline region. This is specifically apparent around and beyond pH 10. We attribute this variability to the chemical reaction between alkali and disulfide bonds in the region [34], namely, beyond pH 10 to form lanthionine and lysinoalanine crosslinks, as reviewed by Bouillon and Wilkinson [10]. The scatter of the data, we specifically attribute to random differences of the chemical performance for individual tress samples and thus to the chemical inhomogeneity of the commercial hair. Together with the literature data, data for both H^+ and OH^- -ions show no consistent trend towards equilibrium uptake within the experimental pH-range.

For both types of conditions our and literature data fall generally within the predicted 95%-confidence limits.

Data points lie on or close to the zero-line in the mid-pH_∞ -range (≈ pH 4–10), traditionally also referred to as 'neutrality' region [15]. In this range, the hair does not seem to absorb neither H^+- nor OH^- -ions [27,4,17,31] and as discussed above.

This observation of an apparent lack of ion-uptake has been considered as evidence that, hair behaves differently with respect to the ion uptake in the mid- compared to the outer- pH-ranges [4]. The effect has, e.g., been attributed to the hindered diffusion for the ions in the mid- pH-range. This in turn has been attributed to the formation of a Donnan-potential related diffusion barrier [15,7]. The point where a perceptible deviation from the zero-line is observed on the acid side is in the range of pH 3–4. This pH-range appears to correspond to the range for the isoelectric point of hair (IEP = 2.5–4.5) ([20]; [21]; [22]).

For the regions of very low and high pHs, the strong increase of ion uptake is generally attributed to the ion absorption by about 800 μM/g each of specific acidic and basic amino acids together with a further small contribution of protein end groups. Specific groups will contribute to the pH-dependence of ion sorption according to their individual pK_A values [4,7,31]. Further effects are expected to derive from chemical reactions (hydrolysis, reactions at disulfide bonds) [10,4,25]. These are considered as minor for the acidic conditions [5]. For alkaline conditions, chemical reactions are regarded as source, namely, for the data scatter in Fig. 6.

At pH < 4 there is a sharp increase of the uptake of H^+-ions (see Fig. 6). Around pH 2 our experimental H^+-uptake values are in the range of 500 μM/g_s, in good agreement with the result of 600 μM/g_s by Bhat et al. [27]. For wool and hair at pH 1 the uptake is in the range of 770–910 μM/g_s, as reviewed by Robbins [4]. This range is generally considered as the maximum acid-binding capacity of hair, namely, on the basis of its content of basic amino acids [15,4,31]. Though the argument to expect a plateau for ion uptake is rather convincing, the experimental evidence for it is rather mixed. For instance, Breuer and Prichard [40] did not find such a plateau but rather determined a further strong increase of H^+ – uptake, when approaching pH 1 (see Fig. 6). This is in line with our (see Fig. 6) as well as literature observations [15].

In the alkaline range and beyond pH 10, a similarly strong upturn of OH^- -uptake is observed. As reviewed by Robbins [4], a maximum uptake of OH^- -ions is estimated to be in the range of 400 μM/g_s with some substantial variations [27,15,4]. In contrast, results by Speakman and Stott [17] and by Steinhard et al. [25,31], in agreement with curves reviewed by Earland [15], rather suggest an exponential increase of OH^- - uptake beyond about pH 11.5. Values of ≈400 μM/g_s at pH 12 and of ≈800 μM/g_s at pH 12.5 were determined, again with substantial variations [25] but in overall satisfactory agreement with the course of the data in Fig. 6.

To describe the data in Fig. 6, traditionally two theoretically models have been applied, namely that of Gilbert and Rideal and of Donnan (reviewed, e.g., by [15,7]). These were later supplemented by alternative theoretical approaches of Oloffson [42] and Breuer [28]. Shortcomings of these approaches and suitable alternatives have been assessed by Lewis and Rippon [26].

In view of the focus of our investigation, we started the analysis of our data with the basic and plausible assumption that, for e.g. acidic conditions, the distribution of H^+-ions between the solid hair and its aqueous environment at any equilibrium pH-conditions is described by Nernst's distribution law [43]. This leads to the partition ratio for H^+ (K_D^H) as:

$$K_D{}^H = [H^+]_S/[H^+]_L \tag{2}$$

$[H^+]_S$ (unit: μM/g_s) is the H^+-uptake of 1 g of hair (solid) and determined from $[\Delta H^+]$ (see Fig. 6). $[H^+]_L$ (unit: μM/g_L) is the equilibrium concentration of H^+-ions in 1 g of the aqueous solution (liquid), as derived from pH_∞ and assuming a density of 1 g/cm^3 for the liquid. All of our considerations implicitly assume electro-neutrality for the system, that is, associated anions (Cl^-) and cations (Na^+) diffuse together with H^+ and OH^-, respectively [7].

Eq. (2) is formally consistent with the classical Donnan equation [44,45]. This assumes a constant ratio of H^+- or OH^--concentrations in, what is assumed to be, a liquid water phase in hair and the aqueous environment on the other, separated by the hair surface as a membrane. In this context, K_D^H would be equal to the Donnan coefficient λ [44].

With respect to the assumption underlying the Donnan approach, it is worthwhile noting that, studies have shown [46] or imply [47,48,49] that there is no liquid water phase in wool and hair. However, this matter is not quite settled [50,3].

Eq. (2) is also formally consistent with a one-parameter sorption isotherm (Henry isotherm) [51,52], thus describing physi-sorption of the ions by hair from the aqueous environment according to Fig. 1 (A and B).

From Eq. (2) it follows that:

$$log\ K_D{}^H = log\ [H^+]_S – log\ [H^+]_L \tag{3}$$

For $[OH^-]$, we formulate accordingly:

$$K_D{}^{OH} = [OH^-]_S/[OH^-]_L \tag{4}$$

and

$$log\ K_D{}^{OH} = log\ [OH^-]_S – log\ [OH^-]_L \tag{5}$$

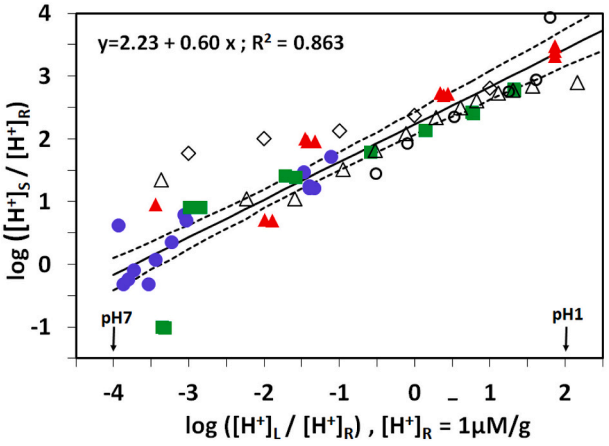

Fig. 7. *log $[H^+]_S$ vs log $[H^+]_L$* for our experimental data in Fig. 6, supplemented by literature data. The markers for the various data sets correspond to those in Fig. 6. The positions on the x-axis, which correspond to pH 7 and pH 1 for HLR-conditions are indicated for orientation. The regression line (solid line), for which the equation is given, corresponds to our experimental data (solid markers) only [29,30]. The line is shown together with its 95%-confidence envelope (broken lines). Details on the parameter values of the linear regression line are given in Table 2. $[H^+]_R$ is a reference concentration, which is applied to remove the concentration units and thus to enable the log-transformation.

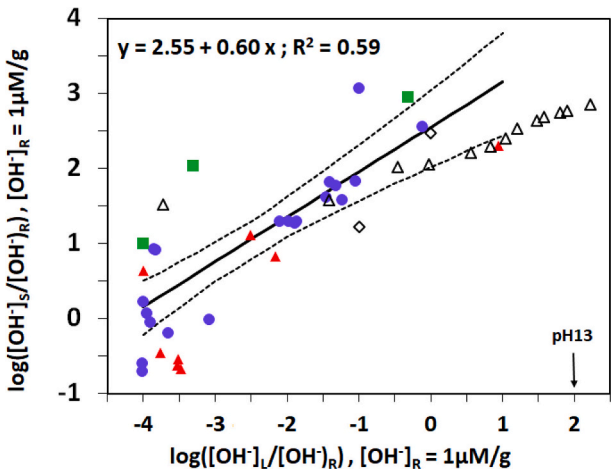

Fig. 8. *log* $[OH_S^-]$ vs *log* $[OH_L^-]$ for our experimental data in Fig. 6. The position on the x-axis, which corresponds pH 13 is indicated for orientation. pH 7 corresponds to x = −4, as in Fig. 7. The regression line (solid line), for which the equation is given, is shown together with its 95%-confidence envelope (broken lines) within the alkaline pH-range. Details of the parameter values are given in Table 2. $[OH^-]_R$ is a reference concentration, which is applied to remove the concentration units and thus to enable the log-transformation.

where OH^- -concentrations have the equivalent meanings and units as $[H^+]$, as given above.

As suggested by the form of Eq. (3), we plot *log* $[H^+]_S$ vs *log* $[H^+]_L$ in Fig. 7 The equivalent plot according to Eq. (5) for $[OH^-]$ is given in Fig. 8.

If K_D^H and K_D^{OH} would have been constant for the whole pH-range, we would have observed straight lines with a slope of unity in Figs. 7 and 8. This is obviously not the case. The results imply that, neither the Donnan- nor alternatively a one-parameter sorption approach (Henry's law) are consistent with the data.

The parameter values for the regression lines in Figs. 7 and 8 are given in Table 2.

All regression parameters are statistically significant well beyond the 95%-confidence level.

The similarity of the regression parameter values (intercept, slope) for H^+ and OH^- in Table 2 is interesting to note. However, we view this as a coincidence, related to the specific experimental conditions. In our case, both acid and base are very strong and fully dissociated and the sole sources of ions in the solution. Their pK_A -values are both well outside the experimental range.

It only requires changes of temperature [25] or addition of an electrolyte ([31]; [53]) to change this special situation and to see strong differential changes of the characteristics of H^+- and OH^- -uptake [54]. Also, substantial changes for ion-sorption have been observed, depending on the strength of acids [55] and bases [24].

Figs. 7 and 8, together with the results in Table 2, support strong linear, two parameter, logarithmic relationships between ion concentrations in the solid and the liquid under equilibrium conditions. This is formally consistent, e.g., with the equation for the Freundlich isotherm [51]. This approach also implies a continuous change of K_D^H with pH.

The results presented in Figs. 7 and 8 thus support the concept of physi-sorption for the ions onto the solid. This provides a fundamentally different approach for the description of $H^+$and OH^- -uptake than pH-based theories [28,15,42,45,56]. The Freundlich-isotherm approach has, e.g., been successfully applied for modelling wool dyeing [57,26].

It is interesting to note that, the suitability of the Freundlich isotherm would also support the notion that there is no truly liquid fraction of water in hair, as discussed above.

Furthermore, in Fig. 7, there are no indications of specific pHs, which may be associated with either the isoelectric point (IEP: 3.4–4.5) [22,21,20] or the isoionic point (IIP: 5.6–6.2) [58]. This implies, that the observation of H^+-uptake is not a suitable method to determine either of these points. Also, Fig. 7 does not support a specific interpretation of the apparent strong uptakes of H^+ − ions for $< \approx$ pH 4 (see Fig. 6).

Finally, the data as well as the linear fit in Fig. 7 provide no basis to expect a plateau for H^+ − uptake within the experimentally feasible pH -range. From this observation, we hypothesise that the range of potential sorption sites provided by the hair proteins is much wider than just specific side groups (plus a minor contribution from end groups) and includes the components of the hydrogen bonds, which are abundant in the keratin proteins [3].

It is interesting to note that this lack of provision for ion equilibrium uptake is already contained in Eq. (2) and thus also an element of the Donnan-theory, in contrast to some of the experimental observations. At this stage, we suggest that, extended experimental work on ion-absorption, as basis for investigating the wide variety of equations for physi-sorption [16,52], may well be suited to assess the plausibility of an equilibrium of ion-uptake within the experimental pH-range.

Analogous considerations, as for H^+ (Fig. 7), apply to OH^- -uptake (Fig. 8). It is worthwhile noting that the coefficient of determination (R^2) for the OH^- -fit is substantially lower than for H^+ (see Table 2), due to the high variability of the *log*$[OH^-]s$ –data.

H^+ − uptake can largely be considered as physi-sorption. The effect is reversible and the H^+- ions may be removed by dialysis (washing) of the hair, as is standard practice for hair grooming processes [59]. The same applies in principle for OH^-. However in this case, physi- is increasingly combined with chemi- sorption, namely, at pH 10 and beyond. The most prominent chemical process is the reaction of the hydroxyl-ion with disulfide bonds to form, e.g., lanthionine. This is a well known reaction for keratins [10,15] which recently was comprehensively reviewed and re-investigated for wool by Abou Taleb et al. [34]. We consider this chemical process as being responsible for the strong temperature-dependence of OH^-, compared to the physi-sorption mechanism for H^+ − uptake [15,25].

In this context, it is also important to note that, the occurrence of a plateau for OH^- is not compatible with the effects expected from the

Table 2
Parameter (intercept, slope) with standard errors (SE) and 95%-confidence range ($q_{95\%}$) for the straight line fits in Figs. 7 and 8. R^2 = coefficient of determination.

	Intercept			Slope			
Ion	Value	SE	$q_{95\%}$	Value	SE	$q_{95\%}$	R^2
H^+ ($N = 26$)	2.23	0.087	0.18	0.60	0.038	0.078	0.863
OH^- ($N = 28$)	2.55	0.26	0.52	0.60	0.087	0.18	0.59

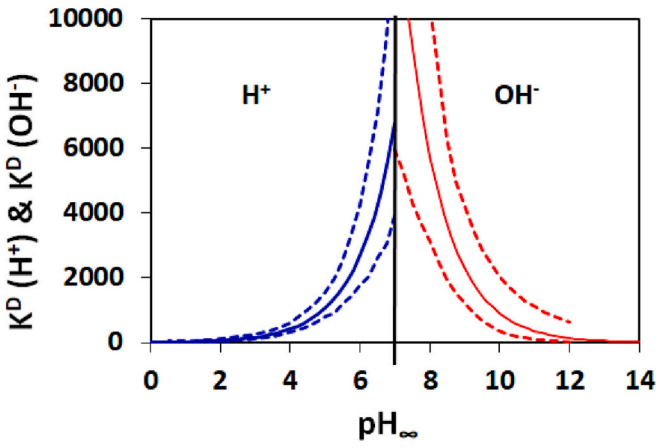

Fig. 9. Partition ratio (K_D) -values for acid and basic equilibrium pH, based on linear regression results in Table 2 (solid lines). 95%-confidence limits (−−) are derived from those in Figs. 7 and 8 (see text).

additional chemi-sorption mechanism. The overall experimental evidence for such a plateau (for wool) is in fact rather mixed.

The linear fits according to Table 2 yield the values for the partition ratio (K_D) across the acidic as well as the alkaline pH-range. The results are summarized in Fig. 9. Error limits for K_D are a combination of those deriving from the components of the fits in Figs. 7 and 8 according to the rules of Gaussian error progression. However, as a matter of simplicity and as basis for a plausible estimate, we consider pH_∞ as an independent variable, so that the 95%-confidence range for K_D is given by that for $[H^+]_S$ and $[OH^-]_S$ (see Figs. 7 and 8). The thus estimated confidence limits for K_D are given in Fig. 9 for both acidic and alkaline conditions. Due to the log → linear transformation, the confidence limits in Fig. 9 are quite large, as to be expected.

The results for the acidic range of Fig. 9 show that, namely when near neutral conditions, there is a strong preference of H^+-ions for the hair. K_D^H reaches a value around $7*10^3$ at pH 7, with rather wide confidence limits (see Fig. 9). The value for K_D^H drops, as to be expected, when $[H^+]$ increases, but still reaches $K_D^H = 27$ at pH 1. Equal concentrations of H^+ − ions in solid and liquid ($K_D^H = 1$) are predicted for around pH -1, well outside the practical and experimental range.

Due to the similarities of the relationships between ion concentration in solid and liquid for the acidic and the basic pH-range (see Table 2), K_D^{OH}-values present somewhat of a mirror image of the acidic range (see Fig. 9). Starting from the numerically higher K_D -value at pH 7 ($K_D^{OH} = 14*10^3$), the values drop to 22 at pH 14. $K_D^{OH} = 1$ lies again well outside the experimental range.

For the whole pH-range, H^+- and OH^- -concentrations are thus always much higher in hair than in the surrounding solution.

These results show that in contrast to general views [4] there is in fact no reduction of relative ion sorption in the mid pH (neutrality) range. Rather to the contrary, bias towards uptake into the hair is especially pronounced between pH 4–7 and pH 7–10, where ion concentrations are relatively low. As to be expected, this absorption bias gets smaller when ion concentrations increase at low and high pHs. In line with considerations above, K_D-values also provide no indication of special roles of certain pHs (IEP, IIP) or amino-acids types across the pH-range. All of these observation and considerations are in line with the suggested behaviour of physi-sorption according to a Freundlich-isotherm.

5. Conclusions

Our study started with a straightforward focus, namely, to study the time-dependent interaction between a pH-adjusted solution and a hair sample. For this we followed traditional protocols, immersing hair samples into an aqueous solutions of known pH and then following the time-dependent pH-changes.

The results show that pH-equilibration across the pH-range follows 1st-order kinetics with a rather long characteristic process time of about 3–5 h. The analysis enables to determine the final uptake of H^+- and OH^- -ions, respectively, for a given pH. The results for the equilibrium uptakes of the ions show that these are not best fitted, as would have been expected from established views, by a one-parameter Donnan- or Henry- but rather by a two-parameter Freundlich -type equation.

In contrast to common views [15,4], this implies that hair acts a strong absorber of H^+- and OH^- -ions across the whole pH-range. This effect is in fact strongest near neutrality. Also, the Freundlich-approach does not provide for a specific fine structure of the sorption isotherm. This justifies to hypothesise, again against common views, that there are no roles for special pHs, for effects of specific groups of amino acids, or of morphological components.

We believe that our approach to investigate the interaction between H^+- and OH^- -ions and hair is thus a feasible tool to provide novel insights into the time-dependent development of the interaction of hair with strong and weak, as well as complex acids and bases.

Building on investigations for wool ([53]; [57,26]), we also expect our approach to facilitate investigations of the effects and application conditions of additives (e.g. salts, surfactants, polymers) on H^+ and OH^--uptake from aqueous solutions used in hair cosmetic products and processes. The Hofmeister-series approach [60] may provide a suitable framework for the analysis and interpretation of such investigations.

Finally, we consider it as worthwhile noting that, our investigation relates only to absorption for H^+ and OH^- by hair. There seems to be little quantitative information about the desorption process (rinsing, dialysis), which may show quite different kinetics as well as pronounced hysteresis effects. In view of the academic as well as potentially significant practical relevance, these would merit further investigation.

CRediT authorship contribution statement

Franz J. Wortmann: Conceptualization, Formal analysis, Methodology, Project administration, Resources, Visualization, Writing – original draft, Writing – review & editing. **Katie Hardie:** Formal analysis, Investigation, Data curation. **Natalja Schellenberg:** Investigation, Data curation, Methodology. **Celina Jones:** Investigation, Project administration. **Gabriele Wortmann:** Conceptualization, Formal analysis, Methodology, Visualization, Data curation, Writing – original draft, Writing – review & editing. **Erik Schulze zur Wiesche:** Conceptualization, Methodology, Resources, Funding acquisition, Writing – review & editing.

Declaration of Competing Interest

FJW and GW are partners in *F & GW – Consultants GbR*. The company provides academic support for the hair cosmetics industry on a consultancy basis.

ESzW is Head of Research & Development at *Dr Kurt Wolff GmbH & Co KG*. In this role he leads, e.g., hair cosmetics R&D at this company.

Acknowledgements

We very much appreciate the financial support of this study by Henkel AG & Co. KGaA (Hamburg) through a split-site PhD-project (NS) as well as through a complementary research project at the University of Manchester (UK).

References

[1] F.J. Wortmann, The structure and properties of wool and hair fibres, in: S. J. Eichhorn, J.W.S. Hearle, M. Jaffe, T. Kikutani (Eds.), Handbook of Textile Fibre Structure, Vol.2: Natural, Regenerated, Inorganic and Specialist Fibres, Woodhead Publ Ltd, Oxford, UK, 2009.
[2] B.S. Lazarus, C. Chadha, A. Velasco-Hogan, J.D. Barbosa, I. Jasiuk, M.A. Meyers, Engineering with keratin: a functional material and a source of bioinspiration, Iscience 24 (8) (2021), 102798.
[3] M. Feughelman, Mechanical Properties and Structure of Alpha-Keratin Fibres: Wool, Human Hair and Related Fibres, UNSW Press, Sydney, AU, 1997.
[4] C.R. Robbins, Chemical and Physical Behavior of Human Hair, Springer, New York, USA, 2012.
[5] J.H. Bradbury, The structure and chemistry of keratin fibers, Adv. Protein Chem. 27 (1973) 111–211.
[6] C. Popescu, F.J. Wortmann, Wool–structure, mechanical properties and technical products based on animal fibres, in: J. Muessig (Ed.), Industrial Applications of Natural Fibres: Structure, Properties and Technical Applications, Chap.12, John Wiley & Sons Ltd, Chichester, UK, 2010, pp. p255–p266.
[7] W.S. Simpson, G. Crawshaw (Eds.), Wool: Science and Technology, The Textile Institute, Woodhead Publ, Cambridge, UK, 2002.
[8] J.B. Speakman, M.C. Hirst, The pH stability region of insoluble proteins, Nature 127 (3209) (1931) 665–666.
[9] J. Jachowicz, M. Berthiaume, M. Garcia, The effect of the amphiprotic nature of human hair keratin on the adsorption of high charge density cationic polyelectrolytes, Colloid Polym. Sci. 263 (10) (1985) 847–858.
[10] C. Bouillon, J. Wilkinson (Eds.), The Science of Hair Care, 2nd edn, Informa Healthcare, London, UK, 2008.
[11] T. Evans, R.R. Wickett (Eds.), Practical Modern Hair Science, Allured Business Media, Carol Stream, IL, USA, 2012.
[12] L. Fernández-Peña, E. Guzmán, Physicochemical aspects of the performance of hair-conditioning formulations, Cosmetics 7 (2) (2020) 26.

[13] S. Hansen, D. Selzer, U.F. Schaefer, G.B. Kasting, An extended database of keratin binding, J. Pharm. Sci. 100 (5) (2011) 1712–1726.
[14] L. Li, S. Yang, T. Chen, L. Han, G. Lian, A measurement and modeling study of hair partition of neutral, cationic, and anionic chemicals, J. Pharm. Sci. 107 (4) (2018) 1122–1130.
[15] C. Earland, in: P. Alexander, R.F. Hudson (Eds.), Wool. Its Chemistry and Physics, 2nd edn, Chapman & Hall Ltd, London, UK, 1963.
[16] Y. Liu, Y.J. Liu, Biosorption isotherms, kinetics and thermodynamics, Sep. Purif. Technol. 61 (3) (2008) 229–242.
[17] J.B. Speakman, E. Stott, The titration curve of wool keratin, Trans. Faraday Soc. 30 (1934) 539–548.
[18] C. Popescu, H. Hoecker, Cytomechanics of hair: basics of the mechanical stability, Int. Rev. Cell Mol. Biol. 277 (2009) 137–156.
[19] N.H. Leon, Structural aspects of keratin fibres, J. Soc. Cosmet. Chem. 23 (1972) 427–445.
[20] V.A. Wilkerson, The chemistry of human epidermis: II. The isoelectric points of the stratum corneum, hair, and nails as determined by electrophoresis, J. Biol. Chem. 112 (1) (1935) 329–335.
[21] A.M. Sookne, M. Harris, Electrophoretic studies of wool, Text. Res. J. 9 (12) (1939) 437–443.
[22] H.C. Parreira, On the isoelectric point of human hair, J. Colloid Interface Sci. 75 (1) (1980) 212–217.
[23] J.B. Speakman, E. Stott, The acid-combining capacity of wool, Trans. Faraday Soc. 31 (1935) 1425–1432.
[24] J. Steinhardt, E.M. Zaiser, Combination of wool protein with cations and hydroxyl ions, J. Biol. Chem. 183 (2) (1950) 789–802.
[25] J. Steinhardt, C.H. Fugitt, M. Harris, Combination of wool protein with acid and base: the effect of temperature on the titration curve, Text. Res. J. 11 (2) (1940) 72–94.
[26] D.M. Lewis, J.A. Rippon (Eds.), The Coloration of Wool and Other Keratin Fibres, John Wiley & Sons and Society of Dyers and Colourists, Bradford, UK, 2013.
[27] R.M. Bhat, R.M. Parreira, E.R. Lukenbach, D.L. Harper, Acid-base characteristics of human hair: absorption of HCl and NaOH, and the effects on physical properties, J. Soc. Cosmet. Chem. 32 (1981) 393–405.
[28] M.M. Breuer, Acid titration of keratin and its implication regarding keratin structure, Trans. Faraday Soc. 60 (1964) 1003–1009.
[29] N. Focht, Influence of Chemical Hair Treatments on the Structure and the Mechanical Properties of Human Hair, PhD-Dissertation, University of Manchester, UK, 2016.
[30] K. Hardie, Influences of Specific Ions on the Physical and Chemical Structure of Human Hair, s, University of Manchester, UK, 2017.
[31] J. Steinhardt, M. Harris, Combination of wool protein with acid and base: hydrochloric acid and potassium hydroxide. III. Results and discussion, Text. Res. J. 10 (6) (1940) 229–252.
[32] K. Hardie, G. Wortmann, E. Schulze Zur Wiesche, F.J. Wortmann, Investigations of the time-dependence of pH-changes in human hair, in: Proc. 7th Int Conf Appl Hair Sci, TRI/Princeton. Red Banks, NJ, USA, 2016. www.researchgate.net/publication/345312745_Investigations_of_the_time-dependence_of_pH-changes_in_human_hair.
[33] F.J. Wortmann, A. Hullmann, C. Popescu, Water management of human hair, Int. J. Cosmet. Sci. 30 (5) (2008) 388–389. www.researchgate.net/publication/350074563_Water_Management_of_Human_Hair.
[34] M. Abou Taleb, S. Mowafi, C. Vineis, A. Varesano, D.O. Sanchez Ramirez, C. Tonetti, H. El-Sayed, Effect of alkali metals and alkaline earth metals hydroxides on the structure of wool fibers, J. Nat. Fib. 19 (9) (2020) 3351–3364.
[35] G. Adam, P. Laeuger, G. Stark, Physikalische Chemie und Biophysik, Springer-Verlag, Berlin, DE, 2003.
[36] R.A. Scherrer, S.M. Howard, Use of distribution coefficients in quantitative structure-activity relations, J. Med. Chem. 20 (1) (1977) 53–58.
[37] J.P. Simonin, On the comparison of pseudo-first order and pseudo-second order rate laws in the modeling of adsorption kinetics, Chem. Eng. J. 300 (2016) 254–263.
[38] J.H. Zar, Biostatistical Analysis, 3rd edn, Prentice Hall, Upper Saddle River, NJ, USA, 1996.
[39] J. Kielland, Individual activity coefficients of ions in aqueous solutions, J. Am. Chem. Soc. 59 (9) (1937) 1675–1678.
[40] M.M. Breuer, D.M. Prichard, The behaviour of hair at low pH values, J. Soc. Cosmet. Chem. 18 (1967) 643–650.
[41] E. Malinauskyte, P.A. Cornwell, L. Reay, N. Shaw, J. Petkov, Effect of equilibrium pH on the structure and properties of bleach-damaged human hair fibers, Biopolymers 111 (11) (2020), e23401.
[42] B. Olofsson, Theory of ionic absorption on wool keratin, J. Polym. Sci. 12 (1) (1954) 301–308.
[43] N.M. Rice, H.M.N.H. Irving, M.A. Leonard, Nomenclature for liquid-liquid distribution (solvent extraction) (IUPAC Recommendations 1993), Pure Appl. Chem. 65 (11) (1993) 2373–2396.
[44] J. Delmenico, R.H. Peters, Application of the Donnan equilibrium to the distribution of dye and inorganic ions between wool and solutions: part I: inorganic ions, Text. Res. J. 34 (3) (1964) 207–219.
[45] L. Peters, J.B. Speakman, The combination of wool with acids–a quantitative interpretation in terms of the Donnan theory of membrane equilibrium, J. Soc. Dye. Colour. 65 (2) (1949) 63–71.
[46] G.W. West, A.R. Haly, M. Feughelman, Physical properties of wool fibers at various regains- part III: study of the state of water in wool by NMR techniques, Text. Res. J. 31 (10) (1961) 899–904.
[47] C. Popescu, P. Augustin, F.J. Wortmann, The desorption of moisture from wool, J. Therm. Anal. Calorim. 120 (1) (2015) 113–117.
[48] F.J. Wortmann, P. Augustin, C. Popescu, Temperature dependence of the water-sorption isotherms of wool, J. Appl. Polym. Sci. 79 (6) (2001) 1054–1061.
[49] F.J. Wortmann, M. Stapels, R. Elliott, L. Chandra, The effect of water on the glass transition of human hair, Biopolymers 81 (5) (2006) 371–375.
[50] M. Feughelman, A.R. Haly, The physical properties of wool fibers at various regains: part VII: the binding of water in keratin, Text. Res. J. 32 (12) (1962) 966–971.
[51] N. Ayawei, A.N. Ebelegi, D. Wankasi, Modelling and interpretation of adsorption isotherms, Hindawi J. Chem. (2017), https://doi.org/10.1155/2017/3039817, 3039817.
[52] J. Wang, X. Guo, Adsorption isotherm models: classification, physical meaning, application and solving method, Chemosphere 258 (2020), 127279.
[53] R.C. Shah, R.S. Gandhi, Distribution of sodium and chloride ions between modified wools and salt solutions in the neutral region of pH, Text Res. Jl 40 (6) (1970) 508–515.
[54] M. Harris, H.A. Rutherford, The base-combining capacity of wool, Text. Res. J. 9 (7) (1939) 245–252.
[55] J. Steinhardt, C.H. Fugitt, M. Harris, Relative affinities of the anions of strong acids for wool protein, Text. Res. J. 11 (6) (1941) 259–284.
[56] L. Peters, A generalized theory for the combination of acid or alkali with wool keratin, J. Text Inst. Trans. 51 (12) (1960) T1290–T1301.
[57] R. Atav, Thermodynamics of wool dyeing, in: R. Morales-Rodrigues (Ed.), Thermodynamics: Fundamentals and its Application in Science. Chap 10, Intech, HR, 2012.
[58] H. Freytag, Hautbewirkte Aenderungen der pH-Werte waessriger Loesungen, J. Soc. Cosmet. Chem. 15 (1964) 265–279.
[59] K. Diekmann, P. Jany, H. Lipp-Thoben, D. Lück, Friseurfachkunde, 2005, 5. Auflg., B.G. Teubner Verlag, Wiesbaden, DE.
[60] H.I. Okur, J. Hladílková, K.B. Rembert, Y. Cho, J. Heyda, J. Dzubiella, P. Jungwirth, Beyond the Hofmeister series: ion-specific effects on proteins and their biological functions, J. Phys. Chem. B 121 (9) (2017) 1997–2014.